Effect of Cosolvent on the Lateral Order of Spontaneously Formed Amphiphilic Amide Two-Dimensional Crystallites at the Air–Solution Interface

Susan P. Weinbach,† Didier Jacquemain,† Franck Leveiller,† Kristian Kjaer,*,‡ Jens Als-Nielsen,*,‡ and Leslie Leiserowitz*,†

Contribution from the Department of Materials and Interfaces, Weizmann Institute of Science, Rehovot 76100, Israel, and Physics Department, Risø National Laboratory, DK4000 Roskilde, Denmark

Received July 26, 1993®

Abstract: At low temperature (5–12 °C), uncompressed films of insoluble amphiphilic molecules $C_{19}H_{39}X$, where the head group X contains one ($CONH_2$, **1**) or two ($CONHC_2H_4CONH_2$, **2**) amide groups, spontaneously form two-dimensional (2D) crystalline clusters over aqueous subphases containing soluble amide or carboxylic acid molecules. These crystallites were detected and their structures were studied using grazing incidence X-ray diffraction (GID). In the presence of subphases containing carboxylic acid (RCO_2H, R = H, CH_2Cl) at sufficiently high concentrations, a loss of diffraction signal was observed for **1**, while amide and less concentrated acid subphases did not show such a destructive effect. The effect of the subphase solute molecules was understood in terms of the different ways in which the solutes hydrogen bond to the amide head groups of the amphiphiles. Both amide and acid solute molecules can form hydrogen-bonded cyclic dimers with the amide head groups. With an amide subphase, such dimers lead to an extension of the hydrogen-bonding network of the crystallites, and thus enhance its stability, but acid molecules may also bind to the monolayer at low concentrations with less than full occupancy. At high acid concentration, and thus more extensive formation of cyclic dimers between carboxylic acid and amphiphilic amide molecules, repulsive interactions between lone pair electrons on oxygen atoms of bound acid molecules inhibit formation of ordered arrays of these dimers and lead to a lack of diffraction signal. In **2**, the second amide group strengthens the crystallites to the extent that there is no decrease in crystallinity over a 1 M formic acid subphase. The shape of the intensity profiles of the Bragg rods and the specular X-ray reflectivity measurements of **2** indicate formation of molecular trilayers.

The composition of the solution from which a crystal is grown strongly influences the morphology of the crystal and may even determine the mode of crystal packing. This phenomenon has been utilized to engineer crystal morphology[1-3] or induce formation of a desired polymorph.[3] The composition of the solution may be varied by use of additives or by changing the solvent itself.

Primary amide and carboxylic acid solvent molecules interact with an amide crystal face, or an analogous two-dimensional (2D) crystallite, by forming a hydrogen-bonded cyclic mixed dimer with the amide moiety of the monolayer or crystal molecule (Scheme I). Such dimers are conformationally and energetically similar.[1] There is, however, a difference in the manner in which the two types of bound solute molecules interact with neighboring solvent molecules. When the solvent molecules are amides, they form an intermolecular NH···O hydrogen-bonding network which is complementary to the hydrogen-bonding network of the crystal, satisfying all potential hydrogen bonds and forming a bilayer (Scheme I, top). Such bilayers occur in many three-dimensional (3D) structures.[4] Bound carboxylic acid molecules can form an analogous network, but the NH···O hydrogen bonds relating bound amide molecules are replaced by lone pair repulsions between the oxygen atoms on neighboring acid molecules (Scheme I, bottom). Energetically, this involves a replacement of a −7 kcal/mol NH···O hydrogen bond by an O···O repulsion of +2 kcal/mol.[5] Three-dimensional crystals of primary amides grown in the presence of small quantities of carboxylic acids, forming solid solutions, show dramatic changes in the morphology of the (host) amide crystal and selective occlusion of the acid into a subset of molecular sites, which leads to a reduction in crystal symmetry.[6] This has been interpreted as a strong inhibition of growth along the hydrogen-bonding direction of the amides, due to the same type of O···O repulsion.[3,7]

Scheme I

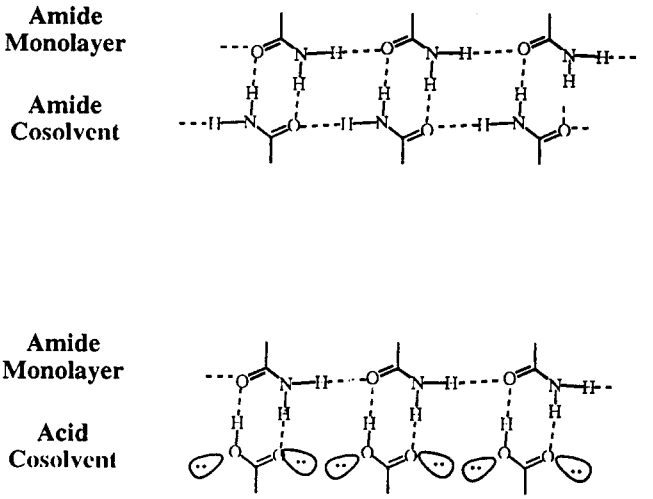

* To whom correspondence should be addressed.
† Weizmann Institute of Science.
‡ Risø National Laboratory.
® Abstract published in *Advance ACS Abstracts,* October 15, 1993.

(1) Addadi, L.; Berkovitch-Yellin, Z.; Weissbuch, I.; van Mil, J.; Shimon, L. J. W.; Lahav, M.; Leiserowitz, L. *Angew. Chem., Int. Ed. Engl.* **1985**, *24*, 466.
(2) Shimon, L. J. W.; Vaida, M.; Addadi, L.; Lahav, M.; Leiserowitz, L. *J. Am. Chem. Soc.* **1990**, *112*, 6215.
(3) Weissbuch, I.; Addadi, L.; Lahav, M.; Leiserowitz, L. *Science* **1991**, *253*, 637.
(4) Leiserowitz, L.; Haglar, A. T. *Proc. R. Soc. London* **1983**, *A388*, 133.
(5) Berkowitz-Yellin, Z.; van Mil, J.; Addadi, L.; Idelson, M.; Lahav, M.; Leiserowitz, L. *J. Am. Chem. Soc.* **1985**, *107*, 3111.
(6) Weisinger-Lewin, Y.; Frolow, F.; McMullan, R. K.; Koetzle, T. F.; Lahav, M.; Leiserowitz, L. *J. Am. Chem. Soc.* **1989**, *111*, 1035.

0002-7863/93/1515-11110$04.00/0 © 1993 American Chemical Society

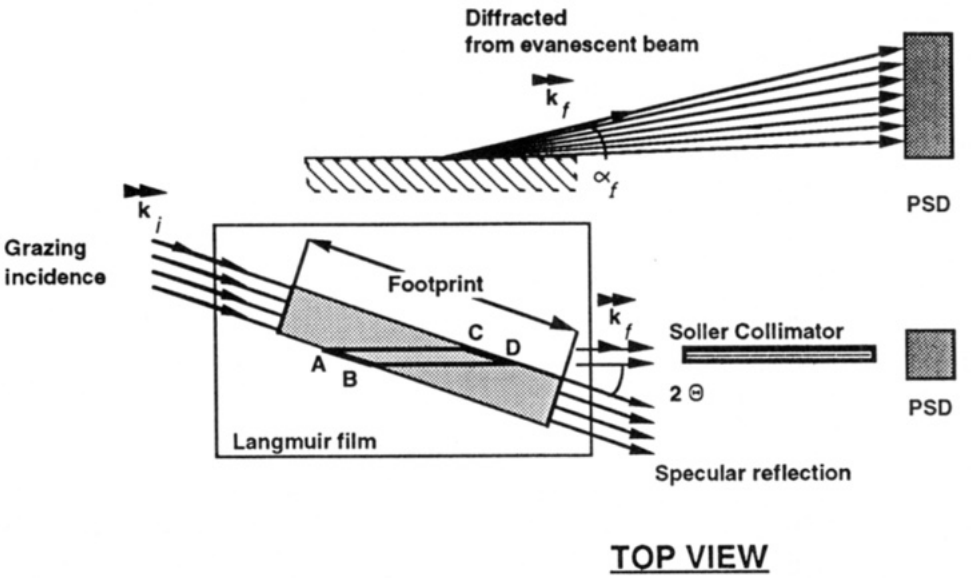

Figure 1. Top and side views of the GID geometry. The footprint of the grazing incidence beam is indicated by the darker area. The position sensitive detector (PSD) has its axis along the vertical direction z. Only the area ABCD contributes to the measured scattering. $\mathbf{k}_i$ and $\mathbf{k}_f$ are incident and outgoing wave vectors. The scattering vector $\mathbf{q}$ is given by $\mathbf{k}_f - \mathbf{k}_i$.

Here we address the question of whether such effects also occur in 2D crystals at the air–solution interface. Monolayers of amphiphilic molecules at the air–solution interface have been used as models to study the effect of a variety of solution additives on 2D crystal growth[8] and structure.[9] Since the hydrophilic side of the film of amphiphilic molecules forms a flat surface in contact with the subphase, such systems allow the study of the equivalent of a single face of a 3D crystal, reducing complications which normally arise from crystal surface roughness or competing growth at adjoining crystal faces. Moreover, at the molecular level, observation of processes at the surface of a 3D crystal surface in contact with solution by direct methods such as grazing incidence X-ray diffraction (GID) is still problematic.[10,11] Crystalline films of amphiphiles, however, are more easily amenable to investigation by GID using synchrotron radiation. This may allow for the direct observation on the molecular level of the effect of molecules dissolved in the subphase at the 2D crystal surface (we refer to a 2D crystal as a *crystallite*). These interactions should be comparable to those of solvent molecules interacting with the faces of 3D crystals.

While 3D crystals are grown from a wide variety of solvents, monolayer experiments have typically been carried out at the air–water interface. In this study, we have investigated the role of acid and amide cosolvents in 2D crystallization, in order to extend the scope of this method and to learn about the role of solvent in crystallite growth and how it compares with the role in 3D crystal growth.

Arachidamide ($C_{19}H_{39}CONH_2$) monolayers were chosen for studying the interaction of solvent with the amide group. GID patterns of this material over pure water and over amide and carboxylic acid solutions were measured. A similar amphiphile incorporating an additional amide group, 3-arachidopropionamide ($C_{19}H_{39}CONHC_2H_4CONH_2$), was also used. The additional hydrogen-bonding network leads to strong intermolecular interactions, which should serve to stabilize the crystallite.

Experimental Section

Arachidic acid (Sigma, purity 99%) was converted into arachidamide in two steps: the formation of the chloride derivative by action of $SOCl_2$ followed by treatment with ammonia. 3-Arachidamidopropionamide was prepared by reaction of arachidic acid with *N*-hydroxysuccinamide with dicyclohexylcarbodiimide in methylene chloride, followed by treatment with 3:1 dimethoxyethene/dioxane and β-alanine, to form 3-arachidamidopropionic acid. This was converted to 3-arachidamidopropanamine by a second reaction with *N*-hydroxysuccinamide, then finally to the amide by use of ammonia and THF. Purities were checked by thin-layer chromatography. The identities of the compounds were checked by NMR and IR.

For the GID measurements, spreading solutions of the arachidamide were prepared in chloroform (Merck, analytical grade), and of 3-arachidamidopropionamide in 95:5 (v/v) chloroform/ethanol, both with concentrations close to 5×10^{-4} M. The monolayers were spread at approximately room temperature over Millipore water before cooling the subphase to 12 ± 1 °C for arachidamide and to 6 ± 1 °C for 3-arachidamidopropionamide.

Grazing Incidence Diffraction. The GID measurements were carried out using the liquid surface diffractometer on beam line D4 at Hasylab, DESY, Hamburg. A sealed and thermostated Langmuir trough equipped with a Wilhelmy balance was mounted on the diffractometer. The films were measured in the uncompressed state, with an average area per molecule of 24 Å^2 for arachidamide and 28 Å^2 for 3-arachidamidopropionamide. The synchrotron radiation beam was monochromated to a wavelength of $\lambda = 1.39$ Å for the arachidamide experiments, and $\lambda = 1.41$ Å for the 3-arachidamidopropionamide experiments, by Bragg reflection from a Ge(111) crystal. This X-ray beam was adjusted to strike the surface at an incident angle of $\alpha = 0.85\alpha_c$, where α_c is the critical angle for total external reflection, to maximize surface sensitivity.[12,13] The angle α_c is equal to 0.138° for arachidamide and to 0.140°

(7) Berkovitch-Yellin, Z.; Addadi, L.; Idelson, M.; Lahav, M.; Leiserowitz, L. *Angew. Chem. Suppl.* **1982**, 1336.
(8) Jacquemain, D.; Grayer Wolf, S.; Leveiller, F.; Deutsch, M.; Kjaer, K.; Als-Nielsen, J.; Lahav, M.; Leiserowitz, L. *Angew. Chem., Int. Ed. Engl.* **1992**, *31*, 130 and references therein.
(9) Weinbach, S. P.; Kjaer, K.; Als-Nielsen, J.; Lahav, M.; Leiserowitz, L. *J. Phys. Chem.* **1993**, *97*, 5200.
(10) It is difficult to extract precise information about interfacial molecular arranagements due to a variety of problems, such as absorption of the X-ray beam by the solvent layer, scattering from the bulk crystal overwhelming that of the surface, and roughness of the 3D crystal–solution interface. Nevertheless, synchrotron radiation has allowed the monitoring of solvent–surface interactions at the crystal–solution interface,[11] but only qualtitative information about the interfacial layer could be obtained.
(11) Cunningham, D.; Davey, R. J.; Roberts, K. J.; Sherwood, J. N.; Shripathi, T. *Journal of Cryst. Growth* **1990**, *99*, 1065.
(12) Als-Nielsen, J.; Kjaer, K. In *Proceedings of the Nato Advanced Study Institue, Phase Transitions in Soft Condensed Matter*, Riste, T., Sherrington, D., Eds.; Plenum Press: New York, Geilo, Norway, 1989; p 113.
(13) Feidenhans, R. *Surf. Sci. Rep.* **1989**, *10* (3), 105.

for 3-arachidamidopropionamide. The dimensions of the footprint (Figure 1) of the incoming X-ray beam on the liquid surface were 50 × 5 mm.

The GID patterns from the 2D crystallite monolayers on the liquid surface arise from a 2D array of Bragg rods,[12-16] which extend parallel to the vertical scattering vector q_z. In general, monolayers composed of crystallites on the water surface are azimuthally randomly oriented and so may be described as "2D powders".[17-21] Thus, the collection of the diffracted radiation using a position sensitive detector (PSD, Figure 1) which intercepted photons over the range $0.0 \leq q_z \leq 1.0$ Å^{-1} was made in two ways. The scattered intensity was measured by scanning over a range along the horizontal scattering vector q_{xy} ($=4\pi \sin \theta/\lambda$, where 2θ is the horizontal angle between the incident and the diffracted beam, as shown in Figure 1) and integrated over the whole q_z-window of the PSD, to yield *Bragg peaks*. Simultaneously, the scattered intensity recorded in channels along the PSD, but integrated over the scattering vector in the horizontal plane across a Bragg peak, produces q_z-resolved scans called *Bragg rod profiles*.

Several different types of information were extracted from the measured profiles. The angular positions 2θ of the Bragg peaks yield the repeat distances $d = 2\pi/q$ for the 2D lattice structure. The Bragg peaks may be indexed by the Miller indices hk to yield the unit cell. The full width at half-maximum of the Bragg peak, FWHM in q_{xy} units, yields the 2D crystalline coherence length L[22] associated with the hk reflection, obtained by shape analysis of the Bragg peak through the Scherrer[23] formula,

$$L \approx (0.9)2\pi/(\mathrm{FWHM}^2 - \Delta^2)^{1/2} \quad (1)$$

where Δ is the resolution of the Soller collimator in q_{xy} units ($\Delta = 0.007$ Å^{-1}). The intensity at a particular value of q_z in a Bragg rod is determined by the square of the molecular structure factor,[12-14,24,25] $|F_{hk}(q_z)|^2$.

Precise information on the molecular chain orientation in the 2D crystal may be obtained from the position of the maxima of the Bragg rods, if the aliphatic tails are uniformly and rigidly tilted in the monolayer. The tilt angle t between the molecular axis and the surface normal is given by[12,14]

$$\cos \psi_{hk} \tan t = q^\circ_z/|q_{hk}| \quad (3)$$

where q°_z is the position of the maximum along the Bragg rod and ψ_{hk} is the azimuthal angle between the molecular tilt direction projected onto the xy plane and the reciprocal lattice vector q_{hk}. The molecules will therefore be perpendicular to the surface when, for all reflections (h,k), q°_z equal 0 Å^{-1}.[12]

Specular X-ray Reflectivity. Specular X-ray reflectivity, as a surface sensitive technique, provides information on the thickness, density, and roughness of a 2D film.[8,26] In addition, it is often possible to obtain information on binding of solute ions or molecules.[27] Specific regions of the observed reflectivity curve are sensitive to specific parameters of the film. When knowledge of these parameters is used, structural information can be extracted from the specular reflectivity curve. For example, the approximate overall thickness of the layer is given by the location of the first intensity minimum corresponding to the first destructive interference. The position of this minimum is, to a first approximation, inversely proportional to the thickness of the layer. For a monolayer, the contrast at this minimum is determined primarily by the density of the polar head groups. The part of the curve at grazing angles below the first intensity minimum is related to the density of the chains. The intensity maximum at higher angles is sensitive to the increased density of the head group of the monolayer due to the binding of ions or of specific solute molecules from the subphase. For multilayer films, the correlation is considerably more complicated. Film roughness results in a continuous decrease in intensity, which becomes more pronounced at higher scattering angles. This roughness may arise from static and thermal diffuseness of the interface.

Results

The GID patterns of the uncompressed film of arachidamide ($C_{19}H_{39}CONH_2$) over pure water and over solutions of amides (0.3 M chloroacetamide and 1 M formamide) and acids (0.3 M chloroacetic acid, 0.3 M formic acid, and 1 M formic acid) are shown in Figure 2a,b. The Bragg rod profiles for arachidamide over a pure water subphase are shown in Figure 3. As can be seen in Figure 2, a change in the subphase strongly affects crystallite formation in the monolayer. This can also be seen from changes in the crystalline coherence lengths L and from the ratios of the relative integrated intensities of the Bragg peaks (Table I). Over pure water, formamide, or dilute formic acid, two peaks are observed. The coherence length of the peak at $q_{xy} = 1.44$ Å^{-1} is greater than 500 Å for all of these systems, while that of the peak at $q_{xy} = 1.52$ Å^{-1} is approximately 200 Å. The formamide and dilute formic acid subphases also lead to a slight change in crystal lattice spacings *versus* those found for pure water. When more concentrated formic acid (1 M) or chloroacetic acid is introduced into the subphase, there is a loss of the diffraction signal due to a lack of crystallinity. There is a substantial change in the ratio of the integrated intensities of the two peaks when moving from pure water to water containing amide or acid cosolvent (Table I), suggesting ordered binding of subphase molecules.

Figure 4 shows the specular X-ray reflectivity curves for uncompressed arachidamide over pure water and over 50% (13 M) formamide. It can be seen that there is a distinct change in the reflectivity curve. The position of the first minimum, which is inversely proportional to the height of the monolayer (see Experimental Section), is at a lower value of q_z than that of the monolayer over pure water, indicating that the molecules are more vertically oriented as a result of binding of formamide molecules. The parameters used in the fittings are shown in Table IV. Note that in both cases the head group box in the two-box model[21,28] includes bound subphase molecules. A possible binding scheme for arachidamide over a water subphase is shown in Scheme II. Binding of formamide to the amphiphilic amide should occur as shown in Scheme I.

Arachidamide was also measured after compression to 26 ± 1 mN/m over all of the subphases discussed (Figure 2c,d). The GID peaks are very broad for all subphases, indicating very small crystalline domains. The peaks are the broadest, and thus the crystallites the smallest, for films over concentrated acids. The crystalline coherence lengths are very anisotropic (Table II). They

(14) Jacquemain, D.; Grayer Wolf, S.; Leveiller, F.; Lahav, M.; Leiserowitz, L.; Deutsch, M.; Kjaer, K.; Als-Nielsen, J. *J. Phys., Colloq.* **1989**, *50*, Suppl. 10, colloque C7, 29.

(15) Vineyard, G. *Phys. Rev. B* **1982**, *26*, 4146.

(16) There is no selection rule or restriction on the component of the scattering vector along the normal to the film, defined as $\mathbf{q}_z$, with magnitude $q_z = 2\pi \sin \alpha_f/\lambda$, where α_f is the angle between the diffracted beam and the water surface, shown in Figure 1. Therefore, the GID patterns from the 2D crystallite monolayers on the liquid surface arise from a 2D array of rods,[12-15] called Bragg rods, which extend parallel to the vector q_z.

(17) Kjaer, K.; Als-Nielsen, J.; Helm, C. A.; Lexhuber, L. A.; Möhwald, H. *Phys. Rev. Lett.* **1987**, *58*, 2224.

(18) Grayer Wolf, S.; Leiserowitz, L.; Lahav, M.; Deutsch, M.; Kjaer, K.; Als-Nielsen, J. *Nature* **1987**, *328*, 63.

(19) Barton, S. W.; Thomas, B. N.; Flom, E. B.; Rice, S. A.; Lin, B.; Peng, J. B.; Ketterson, J. B.; Dutta, P. *J. Chem. Phys.* **1988**, *89*, 2257.

(20) Helm, C. A.; Möhwald, H.; Kjaer, K.; Als-Nielsen, J. *Biophys. J.* **1987**, *52*, 381.

(21) Kjaer, K.; Als-Nielsen, J.; Helm, C. A.; Tippman-Krayer, P.; Möhwald, H. *J. Phys. Chem.* **1989**, *93*, 3200.

(22) The correlation length L associated with the GID $\{h,k\}$ reflection corresponds to the average length of all diffracting crystallites over which "perfect" crystallinity extends in the direction of the reciprocal lattice vector $\mathbf{G}_{hk}$.

(23) Guinier, A. *X-ray Diffraction*; Freeman: San Francisco, 1968.

(24) Leveiller, F.; Jacquemain, D.; Leiserowitz, L.; Kjaer, K.; Als-Nielsen, J. *J. Phys. Chem.* **1992**, *96*, 10380.

(25) The structure factor $F_{hk}(q_z)$ is given by[12-14]

$$F_{hk}(q_z) = \sum_j f_j \exp\{i(\mathbf{q}_{hk}\cdot\mathbf{r}_j + q_z z_j)\} \exp\{-1/2(q_{hk}^2 U_{xy} + q_z^2 U_z)\}$$

where f_j is the scattering factor of the atom j, $\mathbf{r}_j = x_j\mathbf{a} + y_j\mathbf{b}$ is the vector specifying the (x,y) position of the atom j in the unit cell of dimensions a, b, and z_j is the atomic coordinate in angstroms along the vertical direction. The terms U_{xy} and U_z are, respectively, the mean square displacements in each horizontal direction x,y and along the vertical direction z. For the systems examined here, U_{xy} is essentially a constant because the observed reflections are closely spaced. The term U_z was set at 1 Å^2.[24]

(26) Als-Nielsen, J. *X-Ray Reflectivity Studies of Liquid Surfaces*; North Holland: Amsterdam, 1991; Vol. 3.

(27) Daillant, J.; Bosio, L.; Benattar, J. J.; Meunter, J. *Europhys. Lett.* **1989**, *8*, 453.

(28) Parrat, L. G. *Phys. Rev.* **1954**, *95*, 359.

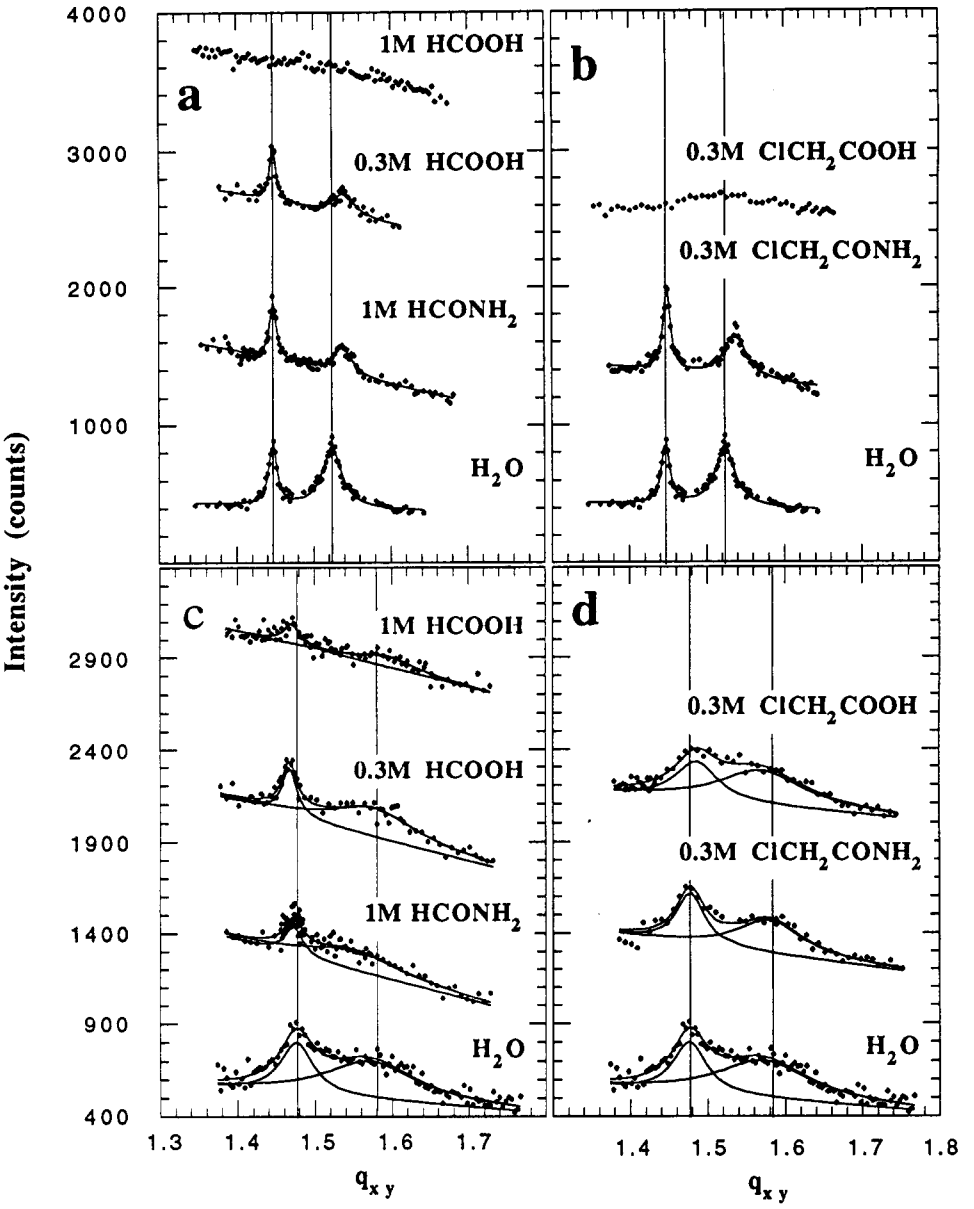

Figure 2. Bragg peaks from GID of (a,b) uncompressed and (c,d) compressed (26 ± 1 mN/M) arachidamide monolayer over aqueous subphases at 12 ± 1 °C. q_{xy} (=$4\pi \sin\theta/\lambda$) is the horizontal scattering vector parallel to the water surface. The solid lines represent the curve fittings used to calculate peak position, integrated intensity, and full width at half-maximum. Vertical lines indicate positions of Bragg peaks over a pure water subphase.

are on the order of about 100–200 Å for the reflection at q_{xy} = 1.48 Å^{-1} and about 50 Å for the reflection at q_{xy} = 1.57 Å^{-1}. This latter value corresponds to *less than 10 lattice spacings*. It is noteworthy that, even in the presence of a concentrated acid subphase, a diffraction signal was observed indicating crystallite formation, although none was observed before compression.

When a second amide is introduced into the chain by use of 3-arachidamidopropionamide ($C_{19}H_{39}CONHC_2H_4CONH_2$), **2**, as the amphiphile, we expect that the binding forces within the crystallites will be strengthened relative to those of arachidamide. The GID patterns of Bragg rods of **2** with three different subphases, *i.e.* pure water, 1 M formamide, and 1 M formic acid, are shown in Figure 5. In this system, there is no pronounced loss of crystallinity over acid or amide solution (Table III), as opposed to that in arachidamide, which contains only a single intermolecular hydrogen-bonding network. For pure water and over a 1 M formic acid subphase, all three observed reflections have associated crystalline coherence lengths which are resolution limited, *i.e.* ≥1000 Å, while over a 1 M formamide solution the weak reflections at q_{xy} = 1.63 Å^{-1} gave a crystalline coherence length of only approximately 300 Å. Clear changes in the relative intensities and in the shapes of the Bragg rod profiles of the reflections at q_{xy} = 1.63 Å^{-1} and q_{xy} = 1.65 Å^{-1} were observed upon change of the subphase (Table III), suggesting binding of the acid and amide subphase molecules.

Discussion

Structure Determination of Uncompressed Arachidamide over a Water Subphase. The two low-order peaks of uncompressed arachidamide over pure water (Figure 2a,b) indicate a rectangular unit cell.[29] It was concluded that the peak at q_{xy} = 1.52 Å^{-1}, which has approximately double the integrated intensity of the peak at q_{xy} = 1.44 Å^{-1}, represents the symmetry-related, coincident {1,1} and {1,$\bar{1}$} reflections, while that at $q_{xy} \approx 1.44$ Å^{-1} represents the {0,2} reflection.[30] From the positions and indexing of the reflections, the unit cell axes were determined to be a = 4.69 Å, b = 8.69 Å. The intensity profile of the low-order {0,2} Bragg rod has its maximum at $q^{\circ}_z \approx 0$ Å^{-1}, indicating that the molecular axis lies in a plane approximately perpendicular to the long b axis

(29) Jacquemain, D.; Leveiller, F.; Weinbach, S.; Lahav, M.; Leiserowitz, L.; Kjaer, K.; Als-Nielsen, J. *J. Am. Chem. Soc.* **1991**, *113*, 7684.
(30) The notation {h,k} refers to both (h,k) and ($\bar{h}$,$\bar{k}$) coinciding reflections.

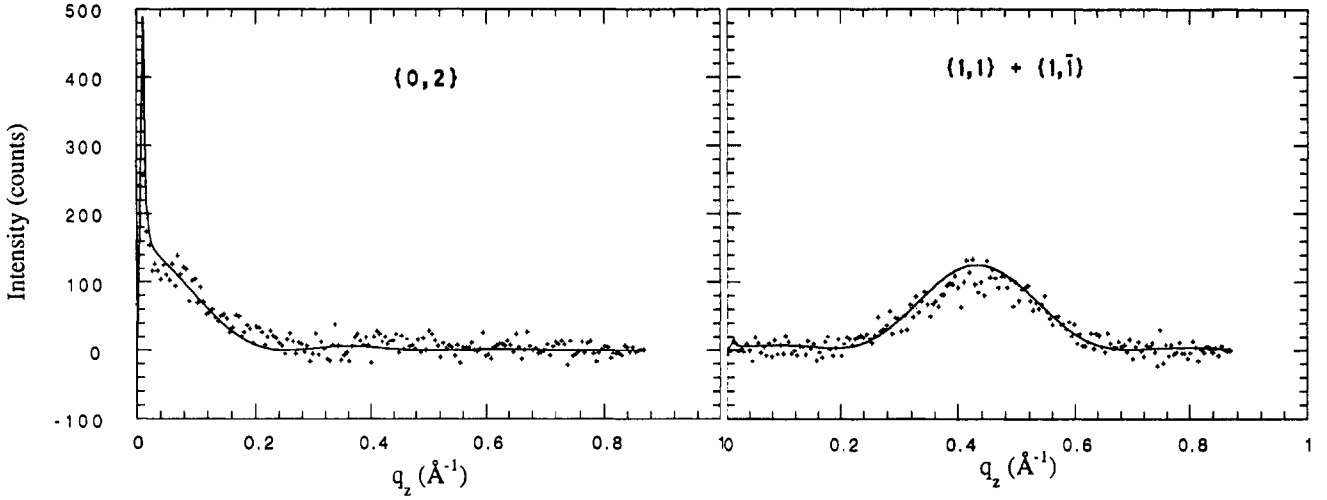

Figure 3. Fitted Bragg rod profiles for the uncompressed arachidamide monolayer over water: (left) {0,2} reflection, q_{xy} = 1.44 Å^{-1}; (right) {1,1} + {1,1̄} reflection, q_{xy} = 1.52 Å^{-1}. The model used in the fittings is shown in Figure 6. The sharp peak observed at around q_z = 0.01 Å^{-1} (q_z is the vertical scattering vector) in the Bragg rods is due to the interference of rays diffracted upward with rays diffracted down and subsequently reflected back up by the interface.[15]

Table I. Grazing Incidence Diffraction Data for Uncompressed Arachidamide over Aqueous Subphases[a]

	{02}				{11} + {1$\bar{1}$}						
subphase	q_{hk}	d	L	q°_z	q_{hk}	d	L	q°_z	$I_{\{02\}}:I_{\{11\}+\{1\bar{1}\}}$	A	a,b
pure water	1.44	4.34	550 ± 60	0	1.52	4.12	190 ± 10	0.4	0.43	20.4	4.69,8.69
1 M formamide	1.44	4.34	680 ± 90	0	1.54	4.08	200 ± 30	0.4	1.1	20.1	4.63,8.68
0.3 M chloroacetamide	1.44	4.34	650 ± 70	0	1.53	4.09	170 ± 10	0.4	0.86	20.1	4.63,8.68
0.3 M formic acid	1.44	4.34	900 ± 180	0	1.54	4.08	180 ± 40	0.4	1.2	20.1	4.63,8.68
0.3 M chloroacetic acid[b]											
1 M formic acid[c]											

[a] The d-spacings are given for each $\{h,k\}$ reflection in units of angstroms; the positional crystalline correlation length associated with the reflection, L, is given in angstroms; q_{hk} and q°_z are given in Å^{-1}. $I_{\{02\}}:I_{\{11\}+\{1\bar{1}\}}$ is the ratio of the integrated intensities of the Bragg peaks. A, the area per molecule = $ab/2$, is given in Å^2. The dimensions of the rectangular unit cell, a,b, are given in angstroms. [b] A single Bragg rod, maximum intensity at q_z = 0, was measured over the entire range of the GID spectrum. [c] No observed diffraction.

Table II. Grazing Incidence Diffraction Data for Compressed Arachidamide over Aqueous Subphases[a]

	{02}			{11} + {1$\bar{1}$}					
subphase	q_{hk}	d	L	q_{hk}	d	L	$I_{\{02\}}:I_{\{11\}+\{1\bar{1}\}}$	A	a,b
pure water	1.48	4.25	110 ± 20	1.57	4.00	40 ± 10	0.6	19	4.5,8.5
1 M formamide	1.47	4.27	220 ± 50	1.55	4.05	50 ± 20	0.4	20	4.6,8.5
0.3 M chloroacetamide	1.48	4.25	140 ± 30	1.58	3.98	60 ± 10	1.0	19	4.5,8.5
0.3 M formic acid	1.47	4.27	250 ± 20	1.58	3.98	50 ± 10	0.3	19	4.5,8.6
0.3 M chloroacetic acid	1.49	4.22	90 ± 20	1.57	4.00	40 ± 10	1.2	19	4.5,8.5
1 M formic acid[b]	1.5	4.2	<100	1.6	3.9	<100		19	4.5,8.5

[a] See note, Table I. [b] Because of the poor quality of the data (Figure 3), a good fit for the GID data was not obtained. The values given are estimates.

Table III. Grazing Incidence Diffraction Data for Uncompressed 3-Arachidamidopropionamide over Aqueous Subphases[a]

	{1$\bar{1}$}				{10}				{01}							
subphase	q_{xy}	d	L	q°_z	q_{xy}	d	L	q°_z	q_{xy}	d	L	q°_z	$I_{1.40}:I_{1.63}:I_{1.65}$	A	a,b	γ
pure water	1.40	4.50	≥1000	0.0	1.63	3.85	≥1000	0.45	1.65	3.80	≥1000	0.51	1.0:1.0:1.0	19.0	5.00,4.94	130
1 M formamide	1.40	4.50	≥1000	0.0	1.62	3.87	≥1000	0.46	1.65	3.80	300 ± 40	0.46	1.0:0.5:1.1	19.1	5.02,4.93	130
1 M formic acid	1.40	4.50	≥1000	0.0	1.62	3.87	≥1000	0.44	1.65	3.80	≥1000	0.45	1.0:0.7:0.8	19.1	5.02,4.93	130

[a] See note, Table I. The ratio of the integrated intensities, $I_{1.40}:I_{1.63}:I_{1.65}$, is calculated from the integrated intensities of the Bragg rod profiles associated with each Bragg peak. The subscripts refer to the position of each peak in q_{xy}. The assignment of the $\{h,k\}$ reflections and the resulting unit cell dimensions correspond to an oblique unit cell (see text). γ is the angle (deg) between the a and b axes of the oblique unit cell.

of the unit cell. The Bragg rod intensity profile of the {1,1} + {1,1̄} reflection is indicative of an 18° tilt from the normal to the water surface, perpendicular to the b axis, using eq 2. A second possibility, in which the assignments of the {0,2} and the {1,1} + {1,1̄} reflections were interchanged, was also considered. In such a case, the unit cell would have axes a = 5.1 Å, b = 8.2 Å. Were this the true unit cell, the Bragg rod for the reflection at q_{xy} = 1.52 Å^{-1} would indicate an arrangement with a molecular tilt of 15° perpendicular to the a axis. This, however, leads to a contradiction, as the {1,1} + {1,1̄} Bragg rod would then have the maximum of its intensity profile at $q^\circ_z \approx 0.2$ Å^{-1}, as calculated according to eq 2, rather than the observed maximum at $q^\circ_z \approx 0$ Å^{-1}.

Having assigned the dimensions of the unit cell, there are now three possible plane groups,[29] $p1g1$, $p11g$, and $c1$.[31] The arrangement of the molecules in plane group $p1g1$, in which the glide is parallel to the b axis, leads to alternation of the direction of the tilt of the chains. This plane group has no systematic

(31) $c1$ denotes a $p1$ structure which we describe for convenience in terms of a centered $c1$ cell with γ nearly equal to 90°.

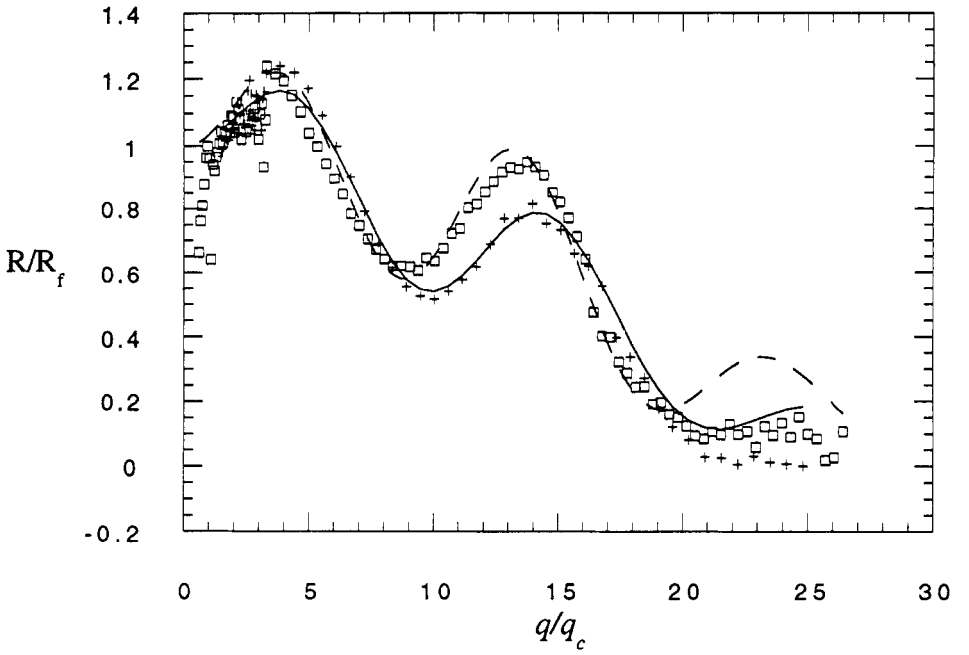

Figure 4. Specular X-ray reflectivity curves for uncompressed arachidamide (+, observed; solid line, fitted) over pure water and (□, observed; broken line, fitted) over 50% formamide. R/R_f is the measured reflectivity divided by the Fresnel reflectivity calculated for a perfect, sharp interface; q_z/q_c is the normalized vertical scattering vector, where q_c is the length of the scattering vector at the critical angle of incidence. The parameters used in the fittings are shown in Table IV.

Table IV. Parameters Used for Fittings of Specular X-ray Reflectivity Data for Arachidamide, Assuming a Two-Box Model[8,26]

	chain			head group			
subphase	electrons	height (Å)	substructure	electrons	height (Å)	substructure	σ (Å)[a]
water	153	21.7	$(CH_2)_{18}CH_3$	43	5.2	$CONH_2 + 2H_2O$	2.7
50% $HCONH_2$	153	24.0	$(CH_2)_{18}CH_3$	47	6.1	$CONH_2 + HCONH_2$	2.6

[a] The root mean square roughness, σ, which is given in angstroms, stems mainly from thermally excited capillary waves on the water surface.[8]

Scheme II

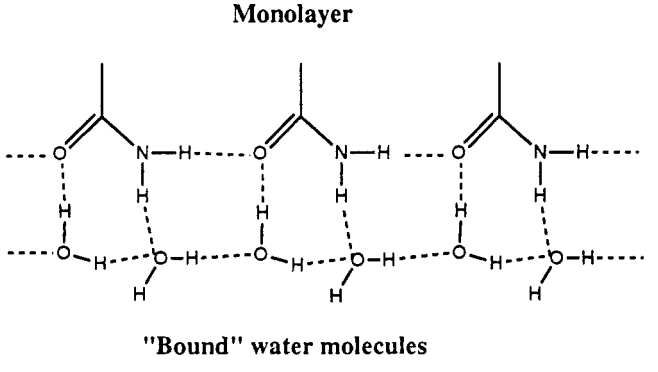

absences for reflections $\{h,k\}$[32] and therefore should give rise to a {1,0} reflection. Structure-factor calculations[12,25] confirm that such a structure would give rise to a strong {1,0} reflection at q_{xy} = 1.34 Å^{-1}. As no peak was found at this position, this packing arrangement was ruled out.

In plane group $p11g$, the glide is parallel to the a axis. In this molecular arrangement, all chain axes are parallel, which would normally lead to a crystal structure in which the planes of the carbon backbones of neighboring chains related by glide symmetry make a herringbone structure. This arrangement is labeled the orthogonal ($O_\perp$) motif[33,34] for long-chain hydrocarbons. When the unit cell, with axes a,b, of a 2D system packing in this arrangement is projected onto a plane perpendicular to the molecular axis, a projected cell a_p, a_b with dimensions $a_p \approx 5.0$ Å, $b_p \approx 7.4$ Å is normally obtained,[29,34] although several exceptions have been observed in which the dihedral angle between the planes of the glide-reflected molecules form an angle of greater than 90°, leading to a projected unit cell having different dimensions.[35,36] In the case of arachidamide, the projected cell has dimensions $a_p = a \cos 18° = 4.46$ Å, $b_p = 8.69$ Å, making this plane symmetry unlikely. In such an arrangement, the symmetry considerations would require that hydrogen bonding be parallel to the 4.69-Å a axis of the unit cell, which is about 0.2–0.3 Å shorter than the translation axis along which primary amides form NH···O bonds in 3D crystals.[4] In the compressed state, the unit cell is of dimensions a = 4.5 Å, b = 8.5 Å, with the molecules aligned vertically. This cell does not have dimensions normally associated with the orthogonal $O_\perp$ motif,[29] although they are not unprecedented. Here the a axis is even shorter, making the possibility of hydrogen bonding parallel to this axis unlikely. Furthermore, a 3:1 mixed monolayer of arachidamide with $C_{19}H_{39}CONHC_2H_4COOH$, which in the uncompressed state packs in a unit cell with the same dimensions as that for arachidamide alone, forms the expected 5.0 Å × 7.4 Å unit cell upon compression,[35] as does an uncompressed longer chain amide, $C_{29}H_{59}CONH_2$.[9] It was therefore assumed that in these two systems the molecules are arranged in the orthogonal $O_\perp$ motif. If one assumes that the presence of the hydrogen-bonding network prevents any change in the plane symmetry of the crystallite upon compression, then the mixed monolayer must have plane symmetry $p11g$ in the uncompressed state as well. Since pure

(32) Henry, N. F. M.; Lonsdale, K. *International Tables for X-ray Crystallography*; Kynoch Press: Birmingham, England, 1965; Vol. 1.

(33) The $O_\perp$ denotes the observation that the planes of the carbon backbones of the glide-related molecules are almost orthogonal to one another.

(34) Small, D. M. In *Handbook of Lipid Research*, Plenum Press: New York, 1986; Vol. 4.

(35) Weissbuch, I.; Majewski, J.; Leveiller, F.; Jacquemain, D.; Kjaer, K.; Als-Nielsen, J.; Leiserowitz, L. *J. Phys. Chem.*, in press.

(36) Leveiller, F.; Böhm, C.; Jacquemain, D.; Möhwald, H.; Leiserowitz, L.; Kjaer, K.; Als-Nielsen, J. Submitted for publication.

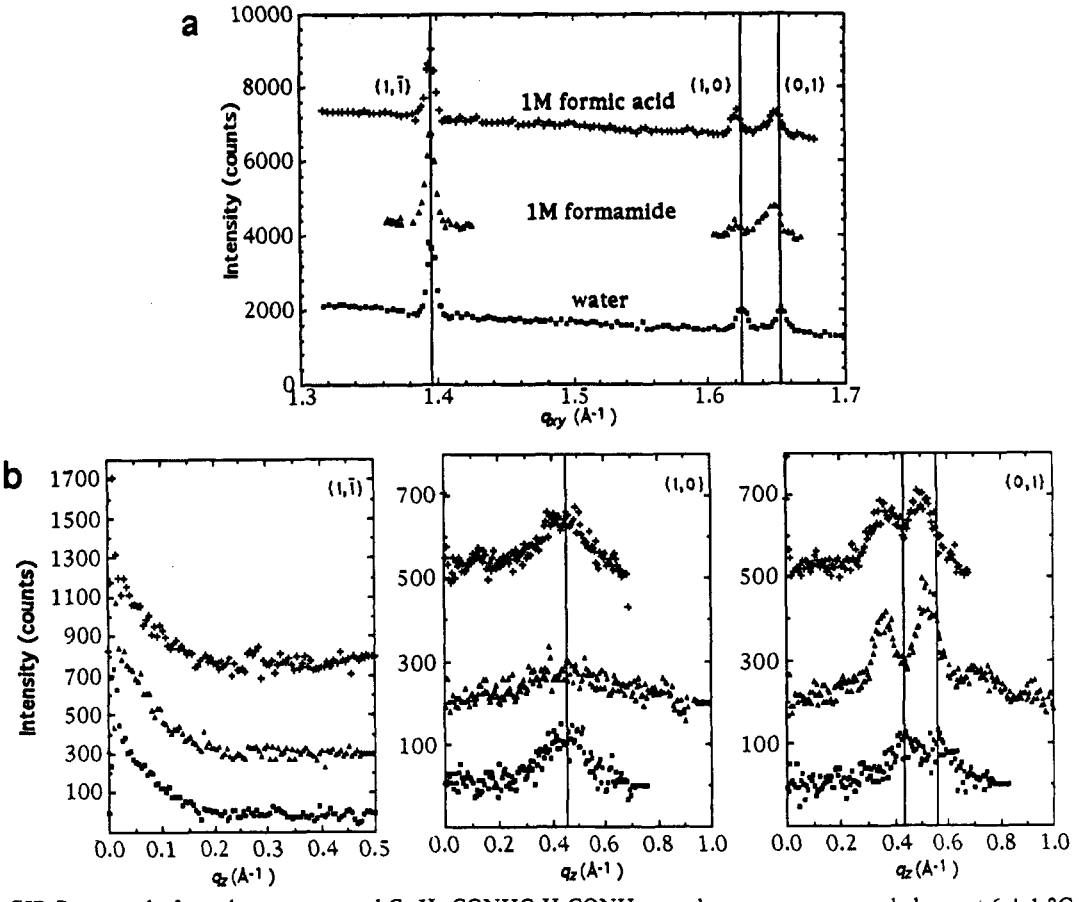

Figure 5. (a) GID Bragg peaks from the uncompressed $C_{19}H_{39}CONHC_2H_4CONH_2$ monolayer over aqueous subphases at 6 ± 1 °C. Note that for these measurements the detector measured only in the range $0 \leq q_z \leq 0.5$ and thus does not include the entire intensities of the reflections at $q_{xy} \approx 1.62$ and $q_{xy} \approx 1.65$. Vertical lines indicate positions of Bragg peaks over a pure water subphase. (b) Intensity profiles along the Bragg rods of the $C_{19}H_{39}CONHC_2H_4CONH_2$ monolayer over aqueous solvents. Note that the Bragg rod for the $(1,\bar{1})$ reflection at $q_{xy} = 1.40$ is plotted on a different scale than the others. Vertical lines indicate positions of maximum intensity along the Bragg rod profiles over a pure water subphase.

arachidamide does not have the expected unit cell upon compression, we assume that it does not have plane symmetry *p*11*g* in the uncompressed state.

We consider the possibility of plane symmetry *c*1,[31] with two molecules per unit cell related only by translation along the unit cell diagonal $^1/_2$(**a** + **b**). The cell of arachidamide projected along the molecular axis, $a_p = 4.46$ Å, $b_p = 8.69$ Å, has dimensions very close to those of the projected cell in the 3D crystal structures of the aliphatic diamides $H_2NOC(CH_2)_nCONH_2$, n = (odd) = 3, 5, 7. In these 3D crystal structures,[37-39] the molecules form (001) layers characterized by a c-centered unit cell. In azelamide (n = 7), for example, the unit cell has dimensions a = 5.78 Å, b = 8.64 Å, γ = 90°. The plane perpendicular to the carbon backbone of the molecule is parallel to the *ac* plane, with the molecular chains in the layer related by translation symmetry only. The molecules are tilted by an angle of 41° *vis-à-vis* the normal to the *ab* plane, leading to the projected cell $a_p = a \cos 41° = 4.36$ Å, $b_p = 8.64$ Å. Rotation of the head group out of the plane of the carbon chain by approximately 25° leads to an NH···O hydrogen-bond network interlinking the molecules *via* translation along the diagonal axis $^1/_2$(**a** + **b**) of length 4.94 Å.

Analysis of the Bragg rod profiles of arachidamide monolayers indicates that the molecules are tilted by 18° from the vertical axis, giving a projected unit cell with a slightly longer projected a_p axis than that of azelamide (4.46 *versus* 4.36 Å), but nearly identical b_p. The carbon chain must be orthogonal to the *ac* plane, as in azelamide, for the intermolecular H···H contacts on either side of the molecule to be equivalent. Indeed, this requirement must be the driving forces for the occurrence of the rectangular unit cell and so for the plane symmetry *c*1, as opposed to *p*1 in which there is no symmetry requirement that γ = 90°. This structural property imposing rectangular symmetry may also be expressed differently. The neighboring CH_2 groups along the carbon chain are related by "local" glide symmetry through the molecule. When this local glide is parallel to the *ac* plane in the rectangular cell, the CH_2 groups along the chain make the same intermolecular contacts in a *c*-centered cell. The amide head groups of arachidamide must be arranged in such a way as to form hydrogen bonds. The 4.69-Å a axis is about 0.2–0.3 Å shorter than the translation axis along which primary amides form NH···O bonds.[4] The unit cell diagonal, $^1/_2|$**a** + **b**| = 4.93 Å, is of the right length for such a bonding network. Upon compression, the unit cell diagonal is of length 4.8 Å. Hydrogen bonding along the 4.69-Å a axis of the uncompressed arachidamide cannot be ruled out, but seems unlikely along the 4.5-Å a axis of the compressed material. In both cases, the unit cell diagonal is closer to the expected length for hydrogen bonding. We therefore propose that hydrogen bonding occurs along this diagonal. This may be accomplished by a rotation of approximately 20° around the C_α–C bond of the $C_\alpha CONH_2$ moiety. The final structure is shown in Figure 6.

Finally, the calculated Bragg rod intensity profiles[25] for the described model for arachidamide over water give a close fit to the observed data, as shown in Figure 3.

Structure of 3-Arachidamidopropionamide (2) over a Water Subphase. Three low-order reflections were measured for this system over each subphase (Figure 5), indicating an oblique cell.[40]

(37) Hospital, M.; Housty, J. *C. R. Hebd. Seances Acad. Sci.* **1965**, *261*, 3820.
(38) Hospital, P. M.; Housty, J. *Acta Crystallogr.* **1966**, *21*, 413.
(39) Hospital, P. M. *Acta Crystallogr.* **1971**, *B27*, 484.

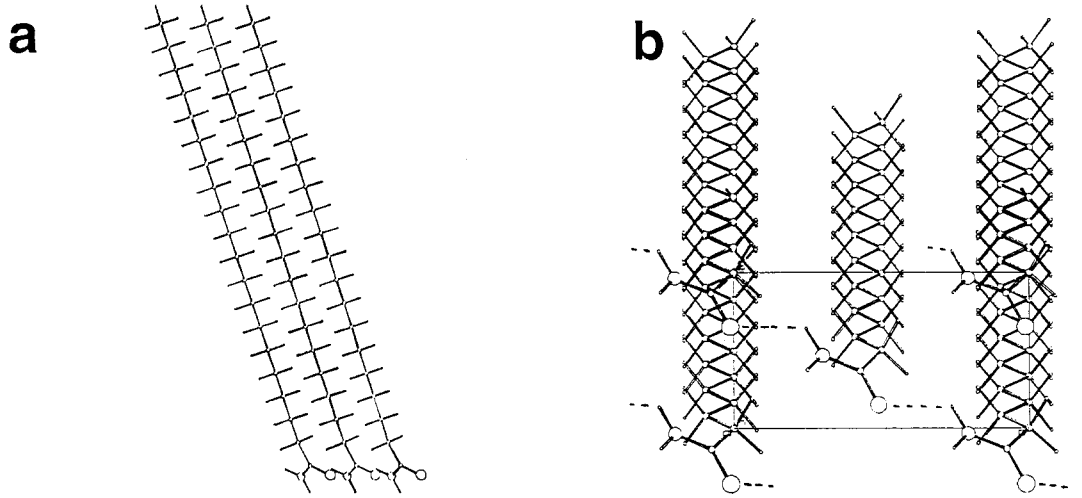

Figure 6. Molecular packing arrangement for arachidamide on a water subphase. The molecules are tilted by 18° from the vertical parallel to the *ac* plane, with the amide groups hydrogen bonded along the unit cell diagonal: (a) view looking along the *b* axis of the unit cell; (b) view perpendicular to the water surface from above. The *ab* unit cell is shown with the *a* axis vertical and *b* horizontal.

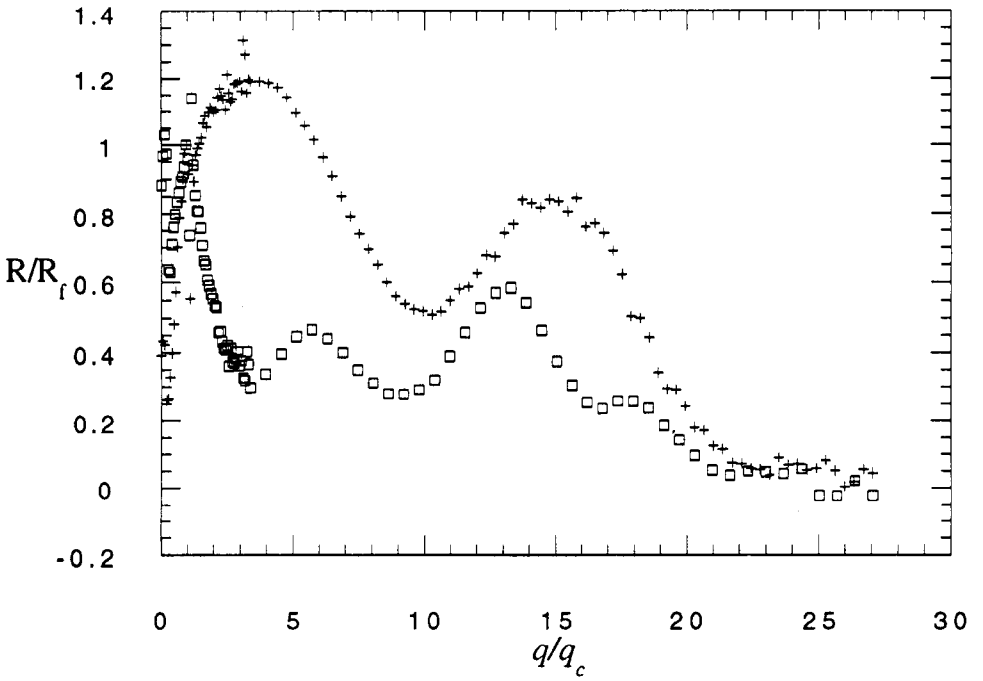

Figure 7. X-ray specular reflectivity of (□) uncompressed 3-arachidamidopropionamide over a water subphase as compared to that of (+) arachidamide under similar conditions.

These three peaks were assigned, in order of increasing q_{xy}, as the $\{1,\bar{1}\}$, $\{1,0\}$, and $\{0,1\}$ reflections, yielding unit cell dimensions $a = 5.02$ Å, $b = 4.93$ Å, $|\mathbf{a} + \mathbf{b}| = 4.24$ Å, $\gamma = 130°$, with an area $ab \sin\gamma$ of 18.96 Å^2, indicating one molecule per unit cell. Both unit cell axes *a* and *b* are the right length for amide hydrogen bonding by translation, probably indicating that one of the two amide groups hydrogen bonds along each axis. The maximum of the Bragg rod profile for the $\{1,\bar{1}\}$ reflection is at the horizon. It can thus be concluded that the molecules are tilted parallel to the (**a** + **b**) axis. The unusually narrow Bragg rod profiles[12] suggest that the film may actually consist of a trilayer, or a trilayer in equilibrium with a monolayer. This deduction is in keeping with the "double-humped" maxima of the Bragg rod profiles for the $\{0,1\}$ and $\{1,0\}$ reflections (Figure 5b) which could not be modeled assuming a monolayer arrangement. Specular X-ray reflectivity measurements confirm this conclusion. It can be seen in Figure 7 that the position of the first minimum in the reflectivity curve of this material over water is at approximately one-third the value in q_z of that for arachidamide over water. The position of this minimum is inversely proportional to the thickness of the film,[21] thus indicating that the film is approximately three times as thick as the arachidamide monolayer. A detailed determination of this structure is currently underway.[41]

Effect of Subphase Molecules on the Amphiphilic Amide Crystallites. The observed loss of crystallinity in uncompressed films of arachidamide in the presence of an acid subphase, but not in an amide subphase, is in line with the difference in binding of the two types of molecules to the amide crystallite (Scheme I), as discussed in the introduction. The repulsive forces between the bound acid molecules, due to repulsions between the lone pair electrons of oxygen atoms on neighboring subphase molecules along the NH···O hydrogen bonding axis $^1/_2$(**a** + **b**), appear to be strong enough to inhibit crystal growth along the (**a** + **b**) direction, while the bound amide has no detrimental effect and, in fact, may actually further stabilize the monolayer due to the

(40) Jacquemain, D.; Grayer Wolf, S.; Leveiller, F.; Deutsch, M.; Kjaer, K.; Als-Nielsen, J.; Lahav, M.; Leiserowitz, L. *Angew. Chem., Int. Ed. Engl.* **1992**, *31*, 130.

(41) Weinbach, S. P. Work in progress.

extension of the hydrogen-bonding network. It is likely that binding of subphase molecules to the long-chain amphiphile molecules occurs more rapidly than self-aggregation and thus influences the initial formation of crystallites. Both acid and amide subphase molecules are able to strongly bind to the amide head groups of such amphiphiles to form mixed dimers (Scheme I). The type of bound subphase molecule within each of these entities strongly influences the ability of the dimers to come together to form crystallites. When the bound subphase molecule is a carboxylic acid, the O···O lone pair repulsions between neighboring carboxyl groups along the (**a** + **b**) diagonal appear to inhibit appropriate positioning of the molecules for crystallite formation. The repulsive forces appear to be sufficient to inhibit crystal formation during the time of the experiment (*ca.* 1.5 h). Even upon compression to 27 mN/m, only a very weak diffraction signal was observed (Figure 2).

3-Arachidamidopropionamide. Once a second amide group has been introduced into the head group of the amphiphile, the doubling of the number of NH···O bonds linking the amphiphilic molecules does overcome the unfavorable O···O interaction imposed by the acid subphase. This can be observed in the case of a 1 M formic acid subphase, which causes a destruction of crystallinity in arachidamide monolayer, but not in 3-arachidamidopropionamide.

Over water alone and over water with 1 M formic acid or 1 M formamide cosolvent, the widths of the Bragg rods and the X-ray reflectivity measurements indicate the formation of trilayer. From the GID data, it can be seen that the cosolvents have a definite effect on the structure of the trilayer. On going from a pure water subphase to 1 M formamide, the ratio of the relative integrated intensities of the reflection at $q_{xy} \approx 1.63$ Å^{-1} relative to that at 1.65 Å^{-1} changes from 1:1 to 1:2. With a pure water subphase, the molecules pack in the oblique cell described above. Because $a \approx b$ (5.02 *versus* 4.93 Å), the unit cell may also be described as *c*-centered pseudorectangular, with $\gamma_r = 88.7°$ and dimensions $a_r = |\mathbf{a} + \mathbf{b}| = 4.21$ Å, $b_r = |\mathbf{a} - \mathbf{b}| = 9.01$ Å. Addition of formamide leads to a decrease in the intensity of the reflection at $q_{xy} = 1.62$ Å^{-1}, thus giving rise to essentially two Bragg peaks. It is possible that this is due to the coexistence of two phases: a minor component with the oblique cell described for a water subphase and a major component with a rectangular unit cell with its two reflections coinciding with two of those of the oblique unit cell. The packing of the molecules in this new phase may be described in terms of a true rectangular unit cell, with dimensions $a = 4.19$ Å, $b = 9.01$ Å, $^1/_2|\mathbf{a} + \mathbf{b}| = 5.03$ Å, and area per molecule 18.9 Å^{-2}. In this rectangular unit cell, the reflections appearing at $q_{xy} = 1.65$ and 1.40 Å^{-1} are reindexed as the {0,2} and the {1,1} + {1,$\bar{1}$} reflections, respectively. Thus, it appears that the intensity of the {0,1} reflection of the phase made up of molecules packed in an oblique unit cell has become weaker, while the intensity of the {1,0} reflection has become stronger. The same effect, although less pronounced, was observed for a 1 M formic acid subphase (Figure 5, Table III).

Conclusion

This report provides evidence for strong subphase effects on the growth of 2D crystallites of hydrogen-bonded monolayer materials in the presence of hydrogen-bonding solutions. The data also indicates the presence of subphase molecules bound to the monolayer in an ordered manner. By using different subphase liquids, "polymorphism" and changes in crystallite growth have been induced. These changes may serve as a model for those induced by changes in the solvent in which 3D crystals are grown. Moreover, it has been shown that a small change in the structure of the monolayer, *i.e.* from one amide to two amides in the chain, induces formation of the trilayer.

Acknowledgment. We thank Ada Yonath of the Max Planck Unit for Structural Molecular Biology for use of laboratory facilities, Christine Böhm for help during the measurements at the synchrotron beam line, and Meir Lahav for useful discussions. We acknowledge financial support from the U.S.–Israel Binational Science Foundation (BSF), the Petroleum Research Fund, administered by the American Chemical Society, the Danish Foundation for Natural Sciences, and HASYLAB, DESY, Hamburg, FRG, for beam time.